BIOCHEMISTRY
including biophysical chemistry & molecular biology

Article

pubs.acs.org/biochemistry

Kinetic Mechanisms of Mutation-Dependent Harvey Ras Activation and Their Relevance for the Development of Costello Syndrome

Michael Wey,[†] Jungwoon Lee,[‡,∥] Soon Seog Jeong,[§] Jungho Kim,[‡] and Jongyun Heo*[,†]

[†]Department of Chemistry and Biochemistry, The University of Texas at Arlington, Arlington, Texas 76019, United States

[‡]Department of Life Science, Sogang University, Seoul 121-742, Korea

[§]Humanzyme, 2201 West Campbell Park Drive, Chicago, Illinois 60612, United States

Supporting Information

ABSTRACT: Costello syndrome is linked to activating mutations of a residue in the p-loop or the NKCD/SAK motifs of Harvey Ras (HRas). More than 10 HRas mutants that induce Costello syndrome have been identified; G12S HRas is the most prevalent of these. However, certain HRas p-loop mutations also are linked to cancer formation that are exemplified with G12V HRas. Despite these relations, specific links between types of HRas mutations and diseases evade definition because some Costello syndrome HRas p-loop mutations, such as G12S HRas, also often cause cancer. This study established novel kinetic parameter-based equations that estimate the value of the cellular fractions of the GTP-bound active form of HRas mutant proteins. Such calculations differentiate between two basic kinetic mechanisms that populate the GTP-bound form of Ras in cells. (i) The increase in the level of GTP-bound Ras is caused by the HRas mutation-mediated perturbation of the intrinsic kinetic characteristics of Ras. This generates a broad spectrum of the population of the GTP-bound form of HRas that typically causes Costello syndrome. The upper end of this spectrum of HRas mutants, as exemplified by G12S HRas, can also cause cancer. (ii) The increase in the level of GTP-bound Ras occurs because the HRas mutations perturb the action of p120GAP on Ras. This causes production of a significantly high population of the only GTP-bound form of HRas linked merely to cancer formation. HRas mutant G12V belongs to this category.

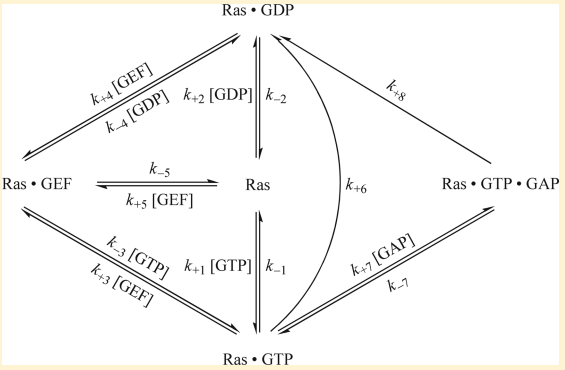

Ras family proteins such as Harvey Ras (HRas), Neuroblastoma Ras (NRas), and Kirsten Ras (KRas) each generate distinct signals despite their interactions with a common set of regulators.[1] These Ras proteins function by cycling between inactive GDP-bound and active GTP-bound states, and various regulators control this GDP−GTP cycling.[2] These regulators include guanine nucleotide exchange factors (GEFs) and GTPase-activating proteins (GAPs).[3] Ras GEFs belong to the positive Ras regulators. Several isoforms of Ras GEFs, including Son of Sevenless (SOS), Ras guanine nucleotide release factor (RasGRF), and Ras guanyl nucleotide-releasing protein (RasGRP), have been identified.[4−6] These GEFs contain a common catalytic core domain Cdc25 and facilitate the intrinsically slow rate of guanine nucleotide exchange (GNE) of Ras-bound GDP/GTP with cellular free GDP/GTP.[7] Because the cellular concentration of GTP is ∼10-fold higher than the concentration of GDP,[8] GEF-mediated Ras GNE populates Ras in their biologically active GTP-bound states. In turn, activated Ras proteins interact with a variety of downstream effector proteins that modulate numerous cellular signaling processes such as cellular proliferation and gene expression.[9] Ras GAPs are the negative Ras regulators. They consist of p120GAP, neurofibromin1 (NF1), and the GAP1 family.[10] All of these Ras GAPs share a RasGAP catalytic core domain.[11] GAPs increase the intrinsically slow rate of GTP hydrolysis for most Ras family proteins to permit conversion of the bound GTP into GDP, thereby terminating Ras downstream signaling.[12]

Several Ras motifs (Figure 1), the phosphate-binding loop (P-loop, Gly^{10}−Ser^{17}), switch I (Gln^{25}−Tyr^{40}), switch II (Asp^{57}−Tyr^{64}), the nucleotide base-binding NKCD (Asn^{116}−Asp^{119}), and SAK (Ser^{145}−Lys^{147}) motifs (HRas numbering), are known to be involved in these binding interactions with GDP and GTP. Many of these Ras motif residues are also directly or indirectly involved in the catalytic functions of GEFs and GAPs (Figure 1).[7,11]

Costello syndrome is a genetic disorder that affects but is not limited to the skin and joints; it also often causes heart abnormalities.[13] Other characteristics are postnatal growth delays, mental retardation, and facial dysmorphism.[13] Mutations in the HRAS gene at codons Gly^{12} and Gly^{13} in the p-loop as well as at Lys^{117} and Ala^{146} in the NKCD and SAK motifs cause the syndrome.[14] The Costello syndrome-relevant HRas mutants for the p-loop Gly^{12} residue include G12A, G12S,

Received: May 29, 2013
Revised: September 25, 2013
Published: November 13, 2013

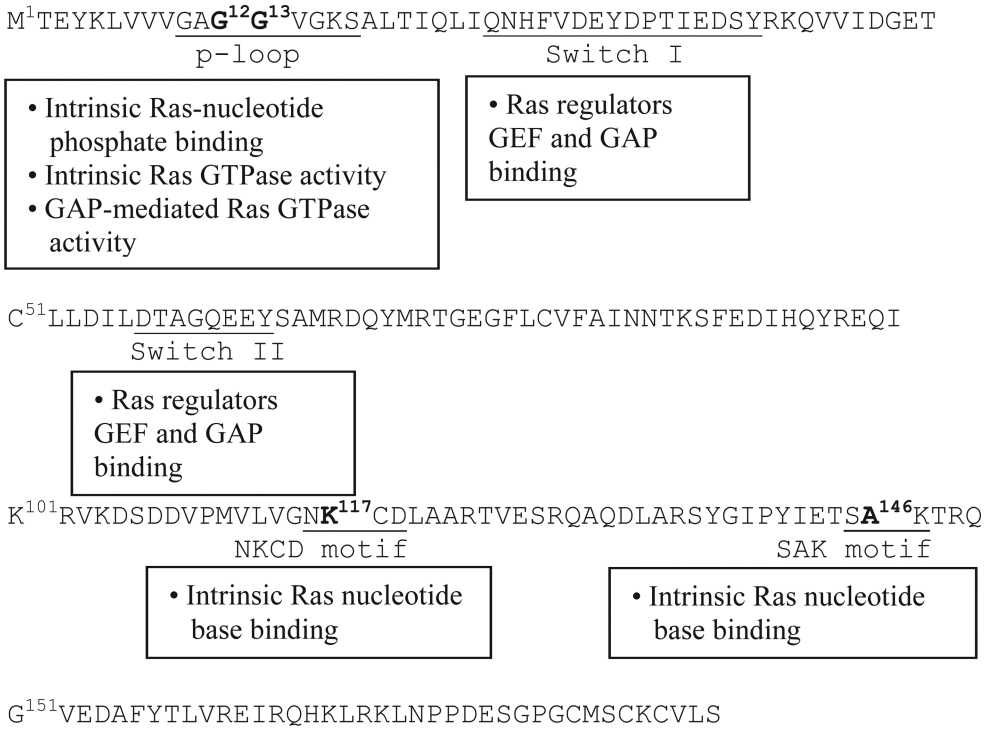

Figure 1. Sequence of wt HRas. The p-loop, switch I, switch II, NKCD, and SAK motifs of wt HRas are underlined. The HRas residues that are known to mutate to produce Costello syndrome-relevant HRas mutants are shown in boldface. These include Gly^{12} and Gly^{13} in the p-loop, Lys^{117} in the NKCD motif, and Ala^{146} in the SAK motif. The boxes depict the contributions of these motifs to the binding and/or catalytic function of Ras with a nucleotide and/or regulators.

G12C, G12D, and G12E (Table 1). Notably, the well-known oncogenic HRas p-loop mutant G12V[15] also causes Costello syndrome (Table 1). Other HRas p-loop mutants that induce Costello syndrome include G13S, G13C, and G13D (Table 1). Symptoms of Costello syndrome also are linked to an unusual HRas NKCD motif K117R mutant and to HRas SAK motif mutants A146T and A146V (Table 1). Of all these HRas mutants, G12S is the most prevalent mutation found in Costello syndrome patients, occurring 5 times more often than other mutations combined (Table 1). When it occurs in NRas and KRas, the G12S mutation often causes certain cancers.[16−18] Because of its weak oncogenicity,[15,19] there has been speculation that G12S HRas is present to serve as a partially active form of HRas to upregulate HRas-dependent cellular signaling.[13] The second most prevalent HRas mutant found in Costello syndrome patients is G12A (Table 1); however, this mutant, unlike G12S, is not commonly found in cancers. Nonetheless, unlike other common HRas p-loop mutants, such as G12V, the biochemical properties of the listed Costello syndrome-relevant HRas mutants (Table 1) have not been fully investigated either with or without their regulators. Accordingly, no definite link has been established between these HRas mutations and the cellular populations of the GTP-bound form of these HRas mutants. This study used the kinetic parameters of Ras and its regulators to formulate novel equations that allow one to estimate the theoretical populations of the GTP-bound Ras in cells. Equipped with these novel equations, this study estimated the values of the theoretical populations of the GTP-bound form of these HRas mutants. The theoretical values were further evaluated with the directly measured cellular populations of the GTP-bound form of selected HRas mutants. These biochemical approaches reveal the kinetic mechanisms by which these HRas mutations contribute to Costello syndrome.

MATERIALS AND METHODS

Protein Preparations. All protein constructs, including wild-type (wt) HRas, p120GAP, and Cdc25, were derived from humans. A full-length wt HRas (residues 1−189) and HRas mutant proteins, including G12V, G12A, G12S, G12C, G12D, G12E, G13V, G13S, G13C, G13D, K117R, A146T, and A146V, were expressed in and purified from *Escherichia coli,* as described in a previous study.[20]

A full-length p120GAP (residues 1−1047) was overexpressed in insect Sf9 cells by using the pIEx vector (Novagen) and then purified using a sequence of columns, including the Sephadex G-150 gel filtration and FPLC Mono-Q columns, as described in a previous study.[21] However, because of the high level of cellular expression of p120GAP, the fast-flow S-Sepharose column step was omitted. The Ras SOS1 catalytic core domain Cdc25 (residues 564−1049) was expressed in and purified from *E. coli*, as described in a previous study.[22]

Kinetic Assay Conditions. All kinetic analyses were performed using >95% pure proteins, as judged by sodium dodecyl sulfate−polyacrylamide gel electrophoresis. The buffer used for all assays consisted of 50 mM NaCl, 10 mM $MgCl_2$, 100 μM diethylenetriaminepentaacetic acid, and 100 mM Tris-HCl (pH 7.4).

Estimation of Kinetic Parameters of Ras GNE in the Presence and Absence of Cdc25. Kinetic parameters of the intrinsic Ras GTP and GDP binding interactions were determined with minor modifications, according to the previously established method.[23] The values of k_{-1}, the intrinsic rate constant for dissociation of GTP from Ras protein, were determined by using the nonhydrolyzable radioactive GTP

dx.doi.org/10.1021/bi400679q | *Biochemistry* 2013, 52, 8465−8479

Table 1. Frequency of HRas Mutations in Costello Syndrome Patients[a]

	Aoki et al.[36]	Gripp et al.[37]	Estep et al.[38]	Kerr et al.[39]	Sol-Church et al.[40]	Zampino et al.[41]	Van der Brugt et al.[42]	Gripp et al.[43]	Burkitt-Wright et al.[44]	Niihori et al.[45]	Digilio et al.[46]	Tidyman et al.[47]	Gripp et al.[48]	Kuniba et al.[31]	Piccione et al.[49]	Schulz et al.[50]	Denayer et al.[51]	Sinico et al.[52]
p-loop mutants																		
G12A	2	2	2	3	2		1			3						3		
G12C				2						1								
G12D										1				1				
G12E				1														
G12S	7	30	30	30	39	8				16	3	4				23		
G12V	1						1		4									
G13C		1	1		1								12		1	1		
G13D	2										1					1		
G13S																		1
G13V[b]																		
NKCD/SAK mutants																		
K117R				1													1	
A146T						1												
A146V								1										
total	12	33	33[c]	37	42	9	4[d]	2[d]	4	21	4	4	12	1	1	31[d]	1	1

[a]Previous reports of the relative occurrence in Costello syndrome of p-loop and NKCD/SAK HRas mutants are summarized. [b]For comparison with Tables 2–4 (see below), G13V HRas is listed. However, the G13V HRas mutant has been linked to cancer, but not to Costello syndrome.[53] [c]In this study, it was noted that 20 of the 33 patients also participated in the investigation conducted by Gripp et al.[37] [d]In these studies, the total number of Costello syndrome patients was noted, but only the relevant HRas mutants were specified.

dx.doi.org/10.1021/bi400679q | Biochemistry 2013, 52, 8465–8479

Scheme 1

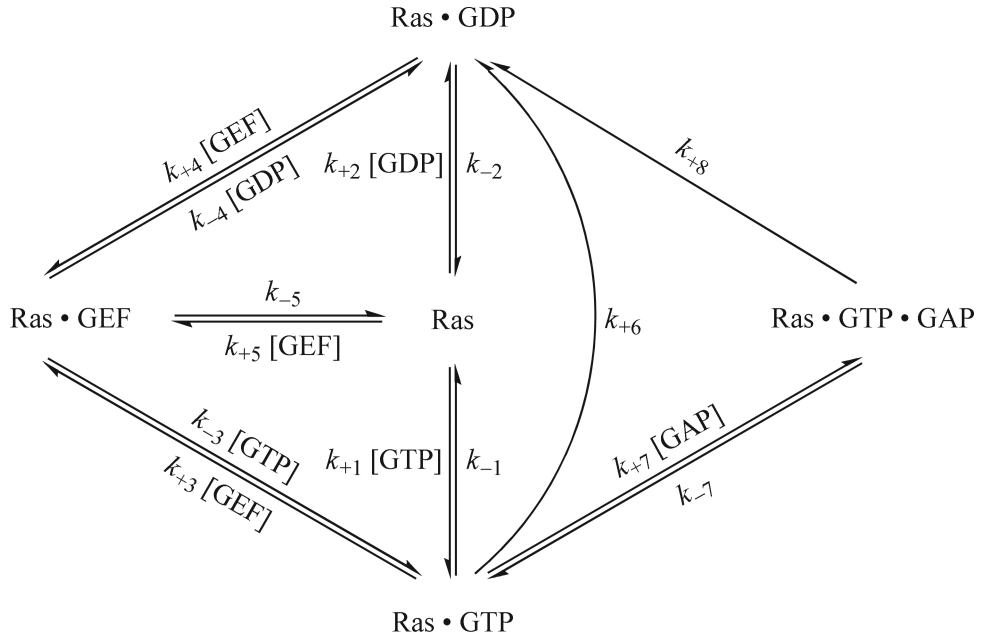

analogue [^{35}S]GTPγS (~400 cpm/pmol) paired with GDP. Ras (1 μM) loaded with [^{35}S]GTPγS was placed in an assay buffer containing GDP (1 μM). Aliquots of the assay mixture were withdrawn at specific intervals over a period of 20000 s and spotted onto nitrocellulose filters. The nitrocellulose filters were washed three times with assay buffer, and the filter-bound radioactivity was measured using a scintillation counter (Beckman LS 6000). These data were fit to single-exponential decays that give values of k_{-1}. The values of k_{-2}, the intrinsic rate constant for dissociation of GDP from Ras proteins, also were measured like k_{-1} were measured, as described above, except that the radioactive [8-^{3}H]GDP (~200 cpm/pmol) paired with GTP was used instead of the [^{35}S]GTPγS paired with GDP.

Kinetic parameters of the Cdc25-mediated Ras-bound GTP and GDP exchange with GDP and GTP were measured as described in a previous study.[22] The values of k_{+3}, the exchange rate constant of the Ras-bound GTP with GDP in the presence of Cdc25, were determined using the 2′(3′)-*O*-(*N*-methylanthraniloyl) 5′-guanylyl-imidodiphosphate (mantGppNHp, a nonhydrolyzable GTP analogue) paired with GDP. In brief, the reaction was initiated by the addition of the various concentrations of the mantGppNHp-loaded Ras (0−500 μM) to an assay buffer containing GDP (5 mM) and Cdc25 (500 nM). Dissociation of mantGppNHp from Ras was monitored over a period of 20000 s by using a fluorescence spectrometer (LS 55, PerkinElmer). These data were fit to a single-exponential decay to determine the apparent rates of dissociation of mantGppNHp from Ras in the presence of Cdc25. Once determined, these rates were then replotted against the concentrations of the mantGppNHp-loaded Ras used. These rates were then fit to a hyperbola to determine the maximal velocity (V_{max}) and the Michaelis−Menten constant (K_M) of the Cdc25-mediated dissociation of mantGppNHp from Ras. According to the Theorell−Chance type of mechanism,[24] the dissociation of GTP from Ras couples with the association of GEF, which is then immediately displaced with GDP (if only GDP is present). Hence, the rate of dissociation of mantGppNHp from Ras represents the exchange rate of mantGppNHp with GDP. Therefore, from the perspective of the Theorell−Chance type of mechanism, the values of V_{max} of the dissociation of the Ras-bound mantGppNHp from Ras per the total Cdc25 enzyme (E_o) are equivalent to k_{+3}. With one exception, the methods and analyses used for the determination of the value of k_{+3} also were applied to determine the values of k_{+4}, the exchange rate constant of the Ras-bound GDP with GTP in the presence of Cdc25. The exception was the use of the 2′(3′)-*O*-(*N*-methylanthraniloyl) guanosine diphosphate (mantGDP) paired with GTP instead of the mantGppNHp paired with GDP.

Estimation of Kinetic Parameters of Ras GTP Hydrolysis in the Presence and Absence of p120GAP. The intrinsic kinetic parameters of Ras GTPase activity were measured, with minor modifications, as described in the previous study.[25] The values of k_{+6}, the rate constant for the intrinsic Ras GTPase activities, were determined by using [γ-^{32}P]GTP (~500 cpm/pmol). As-purified Ras (1 μM) was added to the assay buffer containing [γ-^{32}P]GTP (50 μM). Aliquots were taken from the assay solution at specific intervals over a period of 20000 s and spotted onto nitrocellulose filters. The radioactivity of filtrants that contain only free γ-^{32}P was determined by using a scintillation counter (Beckman LS 6000). The values of k_{+6} were then determined by the fit of these data to a function of exponential decay.

It is of interest that, unlike the GEF-mediated enzymatic process, the GAP-mediated enzymatic process does not follow the Theorell−Chance type of mechanism.[24] This is because the formative process of the Ras·GTP·GAP ternary complex intermediate is not so transient.[11] Nonetheless, within this study, the parameters associated with the p120GAP-mediated Ras GTP hydrolysis were calculated on the basis of the values of K_M and V_{max} of p120GAP for Ras. In brief, the values of k_{+8}, the rate constant for the hydrolysis of GTP of the Ras·GTP·p120GAP ternary complex to produce Ras·GDP, were estimated by dividing V_{max} by the total Ras concentration (E_o); this yields V_{max}/E_o, which is equivalent to k_{cat}, which is the same as k_{+8}. The values of K_M and k_{cat} of p120GAP for Ras were measured by using radioactive [γ-^{32}P]GTP (~500 cpm/pmol)

dx.doi.org/10.1021/bi400679q | *Biochemistry* 2013, 52, 8465−8479

as described in a previous study.[26] As-purified Ras (1 μM) was added to the assay buffer containing [γ-^{32}P]GTP (50 μM) and various concentrations of p120GAP (0−35 μM). Aliquots of the assay mixture were drawn at specific intervals over a period of 20000 s and spotted onto nitrocellulose filters. The radioactivity of only the free ^{32}P-containing liquid filtrants was determined with a scintillation counter (Beckman LS 6000). The apparent rates of Ras GTPase activity in the presence of p120GAP were then determined by the fit of these data to a function of a single-exponential decay. The plots of apparent rates against the concentration of p120GAP that were thus determined were fit to a hyperbola to obtain the values of V_{max} and K_M of p120GAP for Ras GTP hydrolysis.

Comprehensive Kinetic Scheme of Ras Activity Regulation in Cells. Scheme 1 shows a comprehensive web of kinetic paths that describe the regulation of the binding of Ras with its ligands, GTP and GDP. Scheme 1 comprehensively encompasses all of the known cellular kinetic paths that modulate the Ras binding states with GTP and GDP in the presence and absence of Ras regulators, including GEF and GAP. The kinetic parameters denoted in Scheme 1 stand for the kinetic rate constants associated with the processes of the reactions that occur through the kinetic paths. The kinetic parameters shown in Scheme 1 also represent the steps of the reaction processes that occur through the given kinetic paths. According to Scheme 1, three essential kinetic processes in effect determine the featured state of the Ras binding with GTP and GDP. These three are the intrinsic Ras GNE and GTP hydrolysis, the GEF-mediated Ras GNE, and the GAP-mediated Ras GTP hydrolysis in conjunction with the terms of concentration of GTP and GDP ([GTP] and [GDP], respectively). The kinetic steps of k_{+1}, k_{-1}, k_{+2}, and k_{-2} are involved in the intrinsic Ras GNE. The kinetic steps of k_{+3}, k_{-3}, k_{+4}, k_{-4}, k_{+5}, and k_{-5} in combination with the concentration of GEF ([GEF]) are implicated in the GEF-mediated Ras GNE. The kinetic step of k_{+6} is engaged in the intrinsic Ras GTP hydrolysis. The kinetic steps of k_{+7}, k_{-7}, and k_{+8} in combination with the concentration of GAP ([GAP]) are linked to the process of GAP-mediated Ras GTP hydrolysis.

Calculation of the Theoretical Cellular Population of the GTP-Bound Ras. The result of the regulation of Ras binding interactions with GTP and GDP through these paths (Scheme 1) determines the overall comprehensive cellular fraction of the GTP-bound Ras over the GTP- and GDP-bound Ras [the comprehensive $f_{Ras\cdot GTP}$ = [Ras·GTP]/([Ras·GTP] + [Ras·GDP]) of Ras]. The value of the comprehensive $f_{Ras\cdot GTP}$ of Ras is of particular interest because it refers to the overall cellular population of the biologically active form of Ras.

Equation 1 defines the value of the comprehensive $f_{Ras\cdot GTP}$ of Ras that allows the calculation of the theoretical comprehensive cellular population of the GTP-bound form of Ras of interest by using the intrinsic kinetic parameters of Ras as well as the kinetic parameters of GEF and GAP with Ras shown in Scheme 1 (see the Supporting Information for the derivation).

$$\text{comprehensive } f_{Ras\cdot GTP} = \Big[(k_{-2} + k_{+4}[GEF])[GTP]\Big] \Big/ \Big[(k_{-2} + k_{+4}[GEF])[GTP] + (k_{-1} + k_{+3}[GEF])[GDP] + \left(\frac{k_{+7}k_{+8}}{k_{-7} + k_{+8}}[GAP] + k_{+6}\right)([GTP] + [GDP])\Big] \quad (1)$$

Equation 2 expresses the intrinsic cellular fraction of GTP-bound Ras over the GTP- and GDP-bound Ras (the intrinsic $f_{Ras\cdot GTP}$) of Ras in terms of the kinetic parameters of intrinsic Ras GNE and GTP hydrolysis shown in Scheme 1 (see the Supporting Information for the derivation).

$$\text{intrinsic } f_{Ras\cdot GTP} = (k_{-2}[GTP])/[k_{-2}[GTP] + k_{-1}[GDP] + k_{+6}([GTP] + [GDP])] \quad (2)$$

Equation 3 denotes the cellular fraction of GTP-bound Ras over the GTP- and GDP-bound Ras (the GEF-mediated $f_{Ras\cdot GTP}$) of Ras in the presence of GEF in cells shown in Scheme 1 (see the Supporting Information for the derivation).

$$\text{GEF-mediated } f_{Ras\cdot GTP} = [(k_{-2} + k_{+4}[GEF])[GTP]] / [(k_{-2} + k_{+4}[GEF])[GTP] + (k_{-1} + k_{+3}[GEF])[GTP] + k_{+6}([GTP] + [GDP])] \quad (3)$$

Equation 4 expresses the cellular fraction of GTP-bound Ras over the GTP- and GDP-bound Ras (the GAP-mediated $f_{Ras\cdot GTP}$) of Ras in the presence of GAP in cells shown in Scheme 1 (see the Supporting Information for the derivation).

$$\text{GAP-modified } f_{Ras\cdot GTP} = \Big(k_{-2}[GTP]\Big) \Big/ \Big[k_{-2}[GTP] + k_{-1}[GDP] + \left(\frac{k_{+7}k_{+8}}{k_{-7} + k_{+8}}[GAP] + k_{+6}\right)([GTP] + [GDP])\Big] \quad (4)$$

Quantification of Ras-Bound GTP in Cells. Unstimulated NIH 3T3 cells were stably transfected with various HRAS constructs (residues 1−189) using mammalian expression vector pCAGGS with FuGene-6 reagent (Roche). Cells were cultured for 4 days in a complete RPMI 1640 medium and washed with phosphate-free Eagle's minimal essential medium. Resuspended cells were then incubated for 5 h with a serum- and phosphate-free RPMI 1640 medium containing ~50 μCi of ^{32}P/mL. Cells were washed twice with ice-cold PBS (Sigma) and then scraped into an ice-cold homogenization buffer containing 500 mM NaCl, 10 mM $MgCl_2$, 5 mM DTT, 1 mM EDTA, 0.1% Triton X-100, 0.005% SDS, protease inhibitors (0.5 mM phenylmethanesulfonyl fluoride, 1 μg/mL pepstatin A, 1 μg/mL aproptinin, and 1 μg/mL leupeptin), and 10 mM Tris-HCl (pH 7.4). Cells in the ice-cold homogenization buffer were sonified for 4 × 5 s (40 W) on ice followed by centrifugation (100000g) at 4 °C for 20 min. The supernatant

dx.doi.org/10.1021/bi400679q | Biochemistry 2013, 52, 8465−8479

of the cell lysate extract was nutated with Amine Immobilization Resin (Thermo Scientific) coupled with a pan Ras F132 antibody (Santa Cruz Biotechnology) at 4 °C for 5 h. Resin was collected by centrifugation (10000*g*) for 30 min; the proteins bound to the resin were washed with a buffer containing 500 mM NaCl, 10 mM $MgCl_2$, 5 mM DTT, 1 mM EDTA, 0.1% Triton X-100, and 10 mM Tris-HCl (pH 7.4). Nucleotides were eluted from the resin-bound proteins by being treated with a buffer containing 500 mM NaCl, 10 mM $MgCl_2$, 5 mM DTT, 2.5% SDS, and 10 mM Tris-HCl (pH 6.8) at 4 °C for 1 h. The nucleotides were then analyzed by thin-layer chromatography and autoradiographed using densitometry (Bio-Rad GS-670) as described in a previous study[27] to determine the actual cellular fraction of the GTP-bound HRas proteins in the presence of both GEFs and GAPs (cellular $f_{Ras\cdot GTP}$).

RESULTS

The course of this study involved preparation of wt HRas and multitudes of p-loop and NKCD/SAK HRas mutants listed in Table 1. Cdc25 and p120GAP were prepared as GEF and GAP, respectively. The key kinetic parameters (depicted in Scheme 1) of these Ras proteins with and without Cdc25 and/or p120GAP were then determined (Figures 2 and 3). The kinetic values are summarized in Tables 2 and 3. Using eqs 1−4 in conjunction with these values of the kinetic parameters, the intrinsic, GEF- and GAP-mediated, and comprehensive values of $f_{Ras\cdot GTP}$ of these Ras proteins were assessed (Table 4) and analyzed in detail.

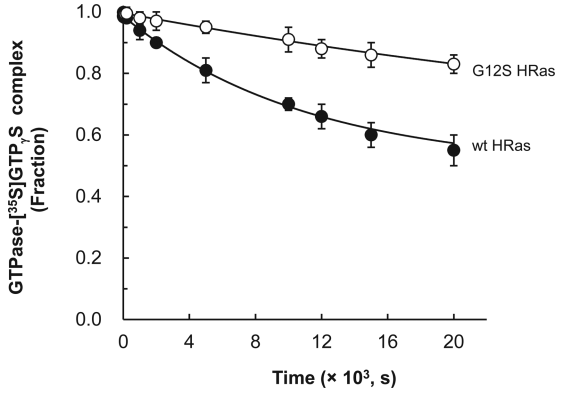

Figure 2. Estimation of the kinetic constants of the intrinsic dissociation of GTP from wt and G12S HRas. Measurements of the rate constants for the Ras GTP dissociation using [^{35}S]GTPγS are described in Materials and Methods. Radioactivity values determined for Ras-bound [^{35}S]GTPγS at various time points were fractionated against the initial radioactivity value of Ras-bound [^{35}S]GTPγS (time zero); the fractionated radioactivity values were plotted vs time. Mean values with the SD of each data point of the plots as derived from three separate independent experiments are shown. Table 2 summarizes the k_{-1} values that were determined by the fit of these plotted values of wt and G12S HRas to a single-exponential decay with regression values (r^2) of >0.9595.

Calculation of the Intrinsic $f_{Ras\cdot GTP}$ Value of Ras. The value of the intrinsic $f_{Ras\cdot GTP}$ of Ras denotes the cellular population of the active GTP-bound form of Ras in the absence of any Ras regulators. A number of the intrinsic $f_{Ras\cdot GTP}$ values of Ras proteins (Table 4) were reached by determination of several kinetic parameters for subsequent calculation in eq 2. These kinetic parameters include (i) the value of the intrinsic GNE of Ras proteins (k_{-1} and k_{-2}) (Table 2) and (ii) the value of the intrinsic GTP hydrolysis of Ras proteins (k_{+6}) (Table 3). This calculation used the previously reported average values of [GTP] (~300 μM) and [GDP] (~40 μM) in human cells.[8]

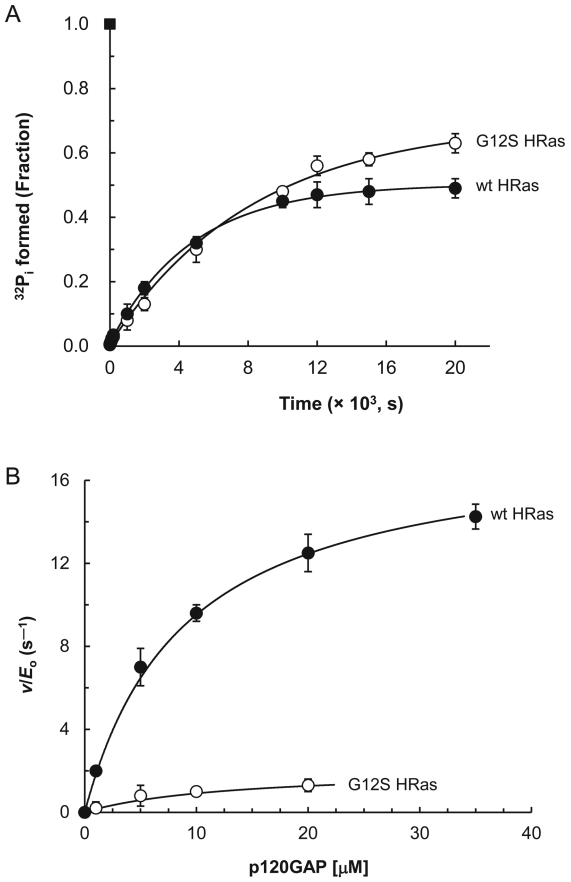

Figure 3. Determination of the kinetic constants for the intrinsic and p120GAP-mediated activities of wt and G12S HRas. Kinetic constants of the phosphatase activity of Ras with and without p120GAP were assessed by using [γ-^{32}P]GTP as described in Materials and Methods. (A) All apparent intrinsic values determined for radioactivity were fractionated against the radioactivity value of [γ-^{32}P]GTP that was initially added to the assay mixture and then plotted vs time. All plot values represent mean values with the SD from three separate independent experiments. The estimated values of k_{+6} as determined by the fit of these plot data to a single-exponential function with an r^2 of >0.9650 are summarized in Table 3. (B) Ras GTPase activity assays in the presence of various concentrations of p120GAP were monitored over a period of time as described in Materials and Methods. The radioactivity values were plotted vs time and fit to a single-exponential function with an r^2 of >0.9965 to determine apparent rates of Ras GTPase activities in the presence of various concentrations of p120GAP. The apparent rates with the SD of Ras GTPase activities were then plotted vs the concentration of p120GAP. All apparent values shown are mean values with the SD from three separate independent experiments. The plots were determined to fit to a hyperbola with an r^2 of >0.9695 to give the V_{max} and K_M values of various Ras proteins coupled with p120GAP for GTP hydrolysis. The V_{max} values were converted into k_{cat} (V_{max}/E_o) values as described in Materials and Methods. The estimated k_{cat} and K_M values are summarized in Table 3.

Analysis of the Intrinsic $f_{Ras\cdot GTP}$ Value of wt HRas. The intrinsic $f_{Ras\cdot GTP}$ value of wt HRas was calculated to be 0.33 (Table 4). The values of k_{-1}, k_{-2}, and k_{+6} of wt HRas (Tables 2 and 3) that determine the intrinsic $f_{Ras\cdot GTP}$ value of wt HRas did

dx.doi.org/10.1021/bi400679q | *Biochemistry* 2013, 52, 8465−8479

Table 2. Kinetic Parameters for the Intrinsic and GEF-Mediated Dissociation of GDP and GTP from wt HRas and Its Mutants[a]

	intrinsic rate constants for Ras nucleotide dissociation ($\times 10^{-4}$ s^{-1})		kinetic parameters associated with Cdc25 ($\times 10^{3}$ s^{-1} M^{-1})	
	GTP dissociation (k_{-1})	GDP dissociation (k_{-2})	GEF-mediated GTP dissociation (k_{+3})	GEF-mediated GDP dissociation (k_{+4})
wt HRas	0.9	1.2	7.2	7.8
p-loop mutants				
G12A	0.9	0.5	7.5	7.3
G12C	0.6	2.2	7.4	8.2
G12D	9.5 (89[d])	1.6 (1.4[d])	7.6	7.0
G12E	4.9	1.5	8.0	7.5
G12S	0.2	4.8	7.0	8.0
G12V	0.9 (0.78[b])	0.2 (0.38[c])	7.5	7.1
G13C	0.8	2.5	7.7	8.2
G13D	6.3	1.6	7.4	7.0
G13S	0.7 (0.83[e])	3.6 (3.83[e])	8.2	8.8
G13V	1.2 (5[e])	3.4 (105[e])	7.4	7.9
NKCD/SAK mutants				
K117R	11.1	13.0 (32[f])	8.6	9.0
A146T	8.1	9.7	8.1	8.2
A146V	9.3	13.5	8.4	8.8

[a]The kinetic values with the SD of the intrinsic dissociation of GTP from wt HRas and G12S were taken from Figure 2. The kinetic values with the SD of the intrinsic dissociation of GTP from all other listed HRas mutants were obtained as described in the legend of Figure 2. In addition, the kinetic values with the SD of the intrinsic dissociation of GDP from these Ras proteins also were obtained as described in the legend of Figure 2, except that [^{3}H]GDP, instead of [γ-^{32}P]GTP, was used. The k_{cat} (V_{max}/E_o) values of the Cdc25-mediated dissociation of the nucleotide from these Ras proteins were obtained by using a saturation kinetic analysis essentially as described in Materials and Methods. A fixed concentration of Ras (1 μM) loaded with either mantGDP or mantGppNHp and variable concentrations of Cdc25 (0−900 μM) was used in this analysis. The values of K_M also were obtained from this saturation kinetic analysis. However, because all determined K_M values of these HRas mutants were indistinguishable from those of wt HRas ($K_M \sim 340$ μM), a listing of the detailed K_M values of these HRas mutants has been omitted. The SDs of the estimated values were within 10% of the values shown. [b]From ref 28. [c]From ref 23. [d]From ref 54. [e]From ref 21. [f]From ref 51.

Table 3. Kinetic Constants for the Intrinsic and p120GAP-Mediated GTPase Activity of wt HRas and Its Mutants[a]

	intrinsic Ras GTP hydrolysis rate (k_{+6}) ($\times 10^{-4}$ s^{-1})	kinetic parameters associated with p120GAP		
		k_{cat} (k_{+8}) (s^{-1})	K_M (μM)	k_{cat}/K_M ($\times 10^{6}$ s^{-1} M^{-1})
wt HRas	2.1	18.0	8.9	2.02
p-loop mutants				
G12A	0.5	0.5	46.8	0.01
G12C	1.8	3.2	12.3	0.26
G12D	1.4 (1.7[b])	0.5	4.8	0.10
G12E	1.6	0.9	4.7	0.20
G12S	1.2	2.1	15.8	0.13
G12V	0.05 (<0.03;[b] 0.33[c])	0.01	<100	~0
G13C	1.1	1.9	26.6	0.03
G13D	1.9	1.3	5.2	0.25
G13S	3.2 (5.33[d])	1.5 (0.5[d])	19.6 (21.6[d])	0.01 (0.023[d])
G13V	2.0 (2.17[d])	0.1	87.0	<0.01
NKCD/SAK mutants				
K117R	1.9	16.2	11.9	1.36
A146T	1.9	12.5	10.7	1.05
A146V	1.8 (same as wt[e])	10.7	13.8	0.78

[a]The kinetic data of the intrinsic and p120GAP-mediated GTPase activities of wt HRas and G12S were taken from Figure 2. Data for other HRas mutants were also collected as described in the legends of Figures 2 and 3. The standard errors of the values were determined to be less than 10% of the values shown. [b]From ref 55. [c]From ref 28. [d]From ref 21. [e]From ref 56.

not deviate significantly from those of the previously reported values.[21,26,28,29]

Analysis of the Intrinsic $f_{Ras\cdot GTP}$ Values of HRas Mutants. All of the intrinsic $f_{Ras\cdot GTP}$ values of the listed HRas mutants exceeded the intrinsic $f_{Ra\cdot GTP}$ value of wt HRas (Table 4).

HRas p-loop mutants G12A and G12V both have k_{-2} values smaller than that of wt HRas but have similar k_{-1} values (Table 2). Although smaller k_{-2} values in eq 2 would suggest a decrease in intrinsic $f_{Ras\cdot GTP}$ values, an increase in intrinsic $f_{Ras\cdot GTP}$ values (Table 4) occurs because of the k_{+6} values in eq 2 that are much smaller than those of wt HRas (Table 3).

Compared with the values of wt HRas, HRas p-loop mutants G12C, G13S, and G13C have a smaller k_{-1} and a larger k_{-2} (Table 2). Nevertheless, these HRas mutants have slightly decreased k_{+6} values compared with the k_{+6} value of wt HRas (Table 3). These combinations of k values in eq 2 favor a value of the intrinsic $f_{Ras\cdot GTP}$ higher than that found for wt HRas.

dx.doi.org/10.1021/bi400679q | Biochemistry 2013, 52, 8465−8479

Table 4. Theoretically Estimated Comprehensive $f_{Ras\cdot GTP}$ Values of wt HRas and Its Mutants[a]

	$f_{Ras\cdot GTP}$ (fraction)							
		GEF-mediated[b]				comprehensive[d]		
	intrinsic	I	II	III	GAP-mediated[c]	I	II	III
wt HRas	0.33	0.39	0.89	0.90	0.01	0.01	0.44	0.89
p-loop mutants								
G12A	0.43	0.55	0.89	0.89	0.19	0.28	0.88	0.89
G12C	0.51	0.55	0.90	0.90	0.07	0.08	0.80	0.90
G12D	0.37	0.42	0.89	0.90	0.10	0.12	0.84	0.90
G12E	0.39	0.44	0.88	0.89	0.06	0.07	0.80	0.89
G12S	0.78	0.79	0.90	0.91	0.23	0.24	0.85	0.91
G12V	0.55	0.74	0.90	0.90	0.46	0.67	0.89	0.90
G13S	0.50	0.52	0.89	0.89	0.23	0.25	0.85	0.89
G13C	0.65	0.68	0.88	0.90	0.21	0.24	0.86	0.90
G13D	0.36	0.40	0.89	0.90	0.05	0.06	0.78	0.90
G13V	0.59	0.61	0.89	0.90	0.54	0.57	0.89	0.90
NKCD/SAK mutants								
K117R	0.79	0.79	0.89	0.90	0.08	0.08	0.57	0.89
A146T	0.76	0.76	0.89	0.90	0.07	0.07	0.58	0.89
A146V	0.81	0.82	0.90	0.90	0.13	0.07	0.58	0.89

[a]The various $f_{Ras\cdot GTP}$ values of wt HRas and its mutants were estimated by using various kinetic parameters (Tables 2 and 3) and eqs 1−4 as described in the Supporting Information. [b]I, minimally active 5 nM Cdc25; II, highly active 5 nM Cdc25; III, highly active 0.6 μM Cdc25. [c]In 10 nM p120GAP. [d]I, minimally active 5 nM Cdc25 with 10 nM p120GAP; II, highly active 5 nM Cdc25 with 10 nM p120GAP; III, highly active 0.6 μM Cdc25 with 10 nM p120GAP.

Another HRas p-loop mutant, G12S, is intriguing, because it has the same trait, a smaller k_{-1} and a larger k_{-2} value versus those of wt HRas, but to a larger extent than HRas mutants G12C, G13S, and G13C (Table 2). G12S HRas also has a slightly increased k_{+6} value compared with the k_{+6} value of wt HRas (Table 3). The combination of these unique k values in eq 2 is reflected in the intrinsic $f_{Ras\cdot GTP}$ value, because G12S has the largest intrinsic $f_{Ras\cdot GTP}$ value, 0.78, among these mutants (Table 4).

HRas p-loop mutants G12D, G13D, and G12E exhibit k_{-1} values much larger than that of wt HRas but display only marginally increased k_{-2} and marginally decreased k_{+6} values compared with those that wt HRas exhibits for the same elements (Tables 2 and 3). However, the intrinsic $f_{Ras\cdot GTP}$ values of these HRas mutants increased slightly in comparison with the values of wt HRas. This is the opposite of the decrease that had been expected (Table 4). This demonstrates again that the k_{-1} value contributes little to the denominator in eq 2 compared with the contribution of k_{-2} and k_{+6}.

The k_{-1} and k_{-2} values of G13V HRas are much higher than the k_{-1} and k_{-2} values of wt HRas (Table 2), but the k_{+6} value of G13V HRas is similar to that of wt HRas (Table 3). The higher k_{-1} and k_{-2} but invariable k_{+6} values indicate the faster Ras GNE. Besides, when the k_{+6} value is unchanged, the higher k_{-1} and k_{-2} values in eq 2 produce a larger intrinsic $f_{Ras\cdot GTP}$ value of Ras. Hence, the larger intrinsic $f_{Ras\cdot GTP}$ value of G13V HRas compared to that of wt HRas (Table 4) reflects the fact that the GNE of G13V HRas is faster than that of wt HRas. This is highlighted again in the case of NKCD/SAK HRas mutants K117R, A146T, and A146V in which the significant change lies in their increased k_{-1} and k_{-2} values, but not in their k_{+6} value, in comparison with those of wt HRas (Tables 2 and 3). This causes the intrinsic $f_{Ras\cdot GTP}$ values of the NKCD/SAK HRas mutants to be nearly twice that of wt HRas (Table 4).

Calculation of the GEF-Mediated $f_{Ras\cdot GTP}$ Value of Ras. The cellular effects of the action of the positive Ras regulator GEFs on Ras proteins were assessed by calculation of the theoretical value of the GEF-mediated $f_{Ras\cdot GTP}$ of Ras (eq 3). The value of the GEF-mediated $f_{Ras\cdot GTP}$ of Ras represents the cellular populations of the active GTP-bound form of Ras in the presence of GEFs. The factors that determine the GEF-mediated $f_{Ras\cdot GTP}$ of Ras are not only GEF-mediated Ras GNE but also intrinsic Ras GNE and GTP hydrolysis. Accordingly, eq 3 consists of the GEF-relevant kinetic terms in addition to the intrinsic kinetic terms that determine the intrinsic $f_{Ras\cdot GTP}$ value. In eq 3, the GEF-relevant kinetic terms are defined as k_{+3} and k_{+4} in combination with [GEF] (i.e., k_{+3}[GEF] and k_{+4}[GEF]).

[GEF] in eq 3 stands for the total cellular concentration of GEFs, such as SOS, RasGRF, and RasGRP. The concentration of the dominantly expressed GEF is vastly different from cell to cell. For example, it has been shown that SOS was dominant in HEK-293T cells at a concentration of 5 nM.[30] In Jurkat T cells, however, the SOS concentration was reported to be 0.6 μM.[31] For the purposes of this study, these two reported dominant cellular levels of SOS were essentially used as [GEF] in eq 3. Although these two reported cases of variations in the levels of SOS expression do not necessarily represent its range of concentration in various cells, they certainly cover a cellularly relevant range of its concentrations from the scope of nanomolar to micromolar.

In this study, the values of the kinetic terms associated with GEF (i.e., k_{+3} and k_{+4}) in eq 3 were determined by using the Cdc25 from SOS. This Cdc25 retains the basal activity of SOS, and thus, these estimated unmodified k_{+3} and k_{+4} values of Cdc25 represent the kinetic parameters of the minimally active SOS. SOS activity in cytoplasm is reported to be increased up to 500-fold by the formation of a complex of SOS with Ras on a plasma membrane.[32] Hence, these values of k_{+3} and k_{+4} multiplied by 500 correspond to the kinetic parameters of the highly active SOS.

Taking into account variations in the levels of cellular expression and activities of SOS permits consideration of three different sets of values of the GEF-relevant kinetic terms. These

dx.doi.org/10.1021/bi400679q | Biochemistry 2013, 52, 8465−8479

are represented by (I) the minimally active 5 nM SOS (designating the action of 5 nM SOS with the original k_{+3} and k_{+4} values), (II) the highly active 5 nM SOS (representing the action of 5 nM SOS with k_{+3} and k_{+4} values multiplied by 500), and (III) the highly active 0.6 μM SOS (denoting the action of 0.6 μM SOS with k_{+3} and k_{+4} values multiplied by 500). Note that the case of the minimally active 0.6 μM SOS is not listed. This is because the values of case II (5 nM SOS with k_{+3} and k_{+4} values multiplied by 500) are equal to the values of the case that includes 0.6 μM SOS with the original k_{+3} and k_{+4} values. Accordingly, we assessed three different values of the GEF-mediated $f_{Ras\cdot GTP}$ of Ras: (i) the GEF-mediated $f_{Ras\cdot GTP}$ of Ras with the minimally active 5 nM SOS [termed the GEF-mediated $f_{Ras\cdot GTP}$ (I) of Ras], (ii) the GEF-mediated $f_{Ras\cdot GTP}$ of Ras with the highly active 5 nM SOS [termed the GEF-mediated $f_{Ras\cdot GTP}$ (II) of Ras], and (iii) the GEF-mediated $f_{Ras\cdot GTP}$ of Ras with the highly active 0.6 μM SOS [termed the GEF-mediated $f_{Ras\cdot GTP}$ (III) of Ras].

Analysis of the GEF-Mediated $f_{Ras\cdot GTP}$ Values of wt HRas. All of the values of the GEF-mediated $f_{Ras\cdot GTP}$ (I), $f_{Ras\cdot GTP}$ (II), and $f_{Ras\cdot GTP}$ (III) of wt HRas, 0.39, 0.89, and 0.90, respectively, were larger than the value of 0.33 of the intrinsic $f_{Ras\cdot GTP}$ of wt HRas (Table 4). This is not too surprising, because the comparison of eqs 2 and 3 predicts that, in general, the presence of the GEF-relevant terms, k_{+3}[GEF] and k_{+4}[GEF], in eq 3 produces a GEF-mediated $f_{Ras\cdot GTP}$ (I) of Ras that is at least similar to or larger than the intrinsic $f_{Ras\cdot GTP}$ value of Ras. Also, eq 3 predicts that a larger value of the GEF-relevant terms produces a larger value of the GEF-mediated $f_{Ras\cdot GTP}$ of wt HRas. Hence, it stands to reason that the GEF-mediated $f_{Ras\cdot GTP}$ (III) of wt HRas has a larger value than the GEF-mediated $f_{Ras\cdot GTP}$ (II) of wt HRas. The same is true for the larger value of the GEF-mediated $f_{Ras\cdot GTP}$ (II) of wt HRas in comparison with the value of the GEF-mediated $f_{Ras\cdot GTP}$ (I) of wt HRas.

Analysis of the GEF-Mediated $f_{Ras\cdot GTP}$ Values of HRas Mutants. Similar to the values associated with wt HRas, the values of the GEF-mediated $f_{Ras\cdot GTP}$ (I) of the listed HRas p-loop mutants were larger than the values of the intrinsic $f_{Ras\cdot GTP}$ of the listed HRas p-loop mutants (Table 4). This is, as with wt Ras, because of the presence of the GEF-relevant terms of these p-loop HRas mutants in eq 3. Intriguingly, among these listed HRas p-loop mutants, G12A and G12V show the largest increases in the GEF-mediated $f_{Ras\cdot GTP}$ (I) values in comparison with intrinsic $f_{Ras\cdot GTP}$ values (Table 4). Nevertheless, such increases exceed expectations. One key contributor to such an increase, in addition to the values of the GEF-relevant terms associated with G12A and G12V HRas, is the particularly small value of k_{-2} of G12A and G12V HRas (Table 2). The presence of a smaller k_{-2} value in eq 3 allows the GEF-relevant terms to weigh more significantly in the determination of the value of the GEF-mediated $f_{Ras\cdot GTP}$ (I) of Ras. The opposite is true of NKCD/SAK HRas mutants K117R, A146T, and A146V. Because these HRas mutants have a much larger k_{-2} value (Table 2), the GEF-relevant terms in eq 3 have relatively little effect on the determination of the value of the GEF-mediated $f_{Ras\cdot GTP}$ (I) of Ras (Table 4).

Unlike the case of the GEF-mediated $f_{Ras\cdot GTP}$ (I) of Ras, the values of the GEF-mediated $f_{Ras\cdot GTP}$ (II) and $f_{Ras\cdot GTP}$ (III) of all of the listed HRas mutants almost uniformly parallel the values of the GEF-mediated $f_{Ras\cdot GTP}$ (II) and $f_{Ras\cdot GTP}$ (III) of wt HRas. These similarities occur because the values of the GEF-relevant terms of these HRas mutants associated with the highly active 5 nM and 0.6 μM SOS were significantly higher than the values of the combined intrinsic kinetic parameters of these HRas mutants in eq 3. As a result, the values of the GEF-mediated $f_{Ras\cdot GTP}$ (II) and $f_{Ras\cdot GTP}$ (III) of these HRas mutants reached their maxima.

Calculation of the GAP-Mediated $f_{Ras\cdot GTP}$ Value of Ras. The cellular consequences of the actions of the negative Ras regulator GAP on Ras were assessed by calculating the theoretical values of the GAP-mediated $f_{Ras\cdot GTP}$ of Ras (eq 4). The value of the GAP-mediated $f_{Ras\cdot GTP}$ of Ras represents the cellular populations of the active GTP-bound Ras in the presence of GAPs.

Equation 4 contains not only the intrinsic kinetic terms that determine the intrinsic $f_{Ras\cdot GTP}$ value but also the GAP-relevant kinetic terms; these include k_{+7}, k_{-7}, and k_{+8} in conjunction with [GAP] [i.e., $k_{+7}k_{+8}/(k_{-7} + k_{+8})$[GAP]]. Intriguingly, the GAP-relevant kinetic terms, $(k_{+7}k_{+8})/(k_{-7} + k_{+8})$, in the denominator of eq 4 are equivalent to the catalytic efficiency, k_{cat}/K_M, of GAP on Ras. Hence, with [GAP], the factors that determine the value of the GAP-mediated $f_{Ras\cdot GTP}$ of Ras that is of interest are those that govern the catalytic efficiency of GAP on Ras.

[GAP] in eq 4 signifies the total concentration of the various types of GAPs in cells. Among these GAPs, p120GAP and NF1 are often dominantly and simultaneously expressed in cells.[33] The kinetic values of k_{cat} and K_M of GAP for Ras (Table 3) were determined by using p120GAP with Ras. Therefore, the GAP-relevant kinetic values listed in Table 3 can be used to assess only the catalytic action of p120GAP, but not NF1, on Ras. The concentration of p120GAP across various mammalian cells, including NIH 3T3 cells, was estimated to be ~10 nM,[33] yet unlike with GEFs (i.e., 0.6 μM SOS), the cellular concentration of p120GAP in the micromolar range has not been reported. Taking these factors into account, we used only one value of the GAP-relevant kinetic terms, the estimated values of k_{cat} and K_M in combination with 10 nM p120GAP, in this study for calculation of the values of the GAP-mediated $f_{Ras\cdot GTP}$ of Ras.

Analysis of the GAP-Mediated $f_{Ras\cdot GTP}$ Value of wt HRas. The estimated GAP-mediated $f_{Ras\cdot GTP}$ value of wt HRas approached 0.01, a value much less than the intrinsic $f_{Ras\cdot GTP}$ value of 0.33 of wt HRas (Table 4). This large difference is due to the magnitude of the value of the GAP-relevant terms, $(k_{+7}k_{+8})/(k_{-7} + k_{+8})$[GAP], which is equivalent to (k_{cat}/K_M)[GAP], added to the denominator in eq 4.

Analysis of the GAP-Mediated $f_{Ras\cdot GTP}$ Values of HRas Mutants. All of the GAP-mediated $f_{Ras\cdot GTP}$ values of these HRas mutants exceeded the GAP-mediated $f_{Ras\cdot GTP}$ value of wt HRas. HRas mutants G12A, G12C, G12D, G12E, G12S, G13C, G13D, and G13S have GAP-mediated $f_{Ras\cdot GTP}$ values that lie between the two extremes of wt HRas and the G12V mutant and also between the two extremes of wt HRas and the G13V mutant (see below) (Table 4). Compared with the values of wt HRas, the values of the GAP-relevant kinetic terms of these mutants are smaller, and thus closer in value to the intrinsic kinetic terms. The decreased catalytic efficiency of p120GAP on these p-loop HRas mutants allows the intrinsic kinetic terms in eq 4 to contribute more to the GAP-mediated $f_{Ras\cdot GTP}$ value compared with what occurs with wt HRas. This contribution by the intrinsic kinetic terms is responsible for the partially active states of these p-loop HRas mutants.

Other p-loop HRas mutants such as G12V and G13V have the largest GAP-mediated $f_{Ras\cdot GTP}$ values. They also have GAP-mediated $f_{Ras\cdot GTP}$ values that changed the least from their

dx.doi.org/10.1021/bi400679q | Biochemistry 2013, 52, 8465−8479

intrinsic $f_{Ras\cdot GTP}$ value. This is because of the miniscule catalytic efficiency of p120GAP on these HRas mutants (Table 3).

Unlike what happens with the p-loop HRas mutants, the catalytic efficiency of p120GAP on the NKCD/SAK HRas mutants K117R, A146T, and A146V does not significantly differ from that of wt HRas (Table 3). However the GAP-mediated $f_{Ras\cdot GTP}$ values of these NKCD/SAK HRas mutants are significantly higher than that of wt HRas (Table 4). The increase in the GAP-mediated $f_{Ras\cdot GTP}$ value is caused by the sufficiently large intrinsic kinetic values of these NKCD/SAK HRas mutants that counteract the values of the GAP-relevant kinetic terms in eq 4 that are associated with these NKCD/SAK HRas mutants.

Calculation of the Comprehensive $f_{Ras\cdot GTP}$ Value of Ras. The effects of the simultaneous actions of both GEF and GAP on Ras were analyzed by calculation of the theoretical value of the comprehensive $f_{Ras\cdot GTP}$ of Ras (eq 1). The comprehensive $f_{Ras\cdot GTP}$ of Ras represents the populations of the active GTP-bound Ras in the presence of both GEF and GAP in cells.

In this study, three different values of the GEF-relevant kinetic terms were used to calculate the GEF-mediated $f_{Ras\cdot GTP}$ values of Ras (see above). For calculation of the GAP-mediated $f_{Ras\cdot GTP}$ values of Ras, only one value of the GAP-relevant kinetic terms was used (see above). Three distinct combinational value sets of the GEF/GAP-relevant kinetic terms are possible. These are represented by (I) the minimally active 5 nM SOS and 10 nM p120GAP, (II) the highly active 5 nM SOS and 10 nM p120GAP, and (III) the highly active 0.6 μM SOS and 10 nM p120GAP. Accordingly, three different sets of the comprehensive $f_{Ras\cdot GTP}$ values of Ras were calculated: the comprehensive $f_{Ras\cdot GTP}$ of Ras with the minimally active 5 nM SOS and 10 nM p120GAP [termed the comprehensive $f_{Ras\cdot GTP}$ (I) of Ras], the comprehensive $f_{Ras\cdot GTP}$ of Ras with the highly active 5 nM SOS and 10 nM p120GAP [termed the comprehensive $f_{Ras\cdot GTP}$ (II) of Ras], and the comprehensive $f_{Ras\cdot GTP}$ of Ras with the highly active 0.6 μM SOS and 10 nM p120GAP [termed the comprehensive $f_{Ras\cdot GTP}$ (III) of Ras]. These values of the comprehensive $f_{Ras\cdot GTP}$ (I), $f_{Ras\cdot GTP}$ (II), and $f_{Ras\cdot GTP}$ (III) of the Ras of interest, including wt, G12V, and G12S HRas, were further used to analyze the corresponding actual values of the fraction of the GTP-bound form (the cellular $f_{Ras\cdot GTP}$) of Ras measured in NIH 3T3 cells.

Analysis of the Comprehensive $f_{Ras\cdot GTP}$ Values of wt HRas. The values of the comprehensive $f_{Ras\cdot GTP}$ (I), $f_{Ras\cdot GTP}$ (II), and $f_{Ras\cdot GTP}$ (III) of wt HRas are 0.01, 0.44, and 0.89, respectively (Table 4). The results suggest that the comprehensive $f_{Ras\cdot GTP}$ value of wt HRas depends largely on the combinational actions of SOS with p120GAP.

The cellular $f_{Ras\cdot GTP}$ value of the transfected wt HRas in unstimulated NIH 3T3 cells was estimated to be 0.12 (Figure 4). Notably, a previously measured cellular $f_{Ras\cdot GTP}$ value of the transfected wt HRas in unstimulated NIH 3T3 cells was reported to be 0.025.[34] One possible reason for such different values would be the different quantification methods used for the GTP- and GDP-bound Ras isolated from cells. The difference in cell culture conditions may also affect the ratio of GTP-bound Ras to GDP-bound Ras. Regardless of the differences in the values, the estimated cellular $f_{Ras\cdot GTP}$ values of the transfected and endogenous wt HRas in unstimulated NIH 3T3 cells fall between the values of the comprehensive $f_{Ras\cdot GTP}$ (I) and $f_{Ras\cdot GTP}$ (II) of wt HRas (Table 4). This is not unexpected because the cellular expression and activity of GEFs and GAPs in unstimulated NIH 3T3 cells would not duplicate the value sets in eq 1 for the calculations of any of these comprehensive $f_{Ras\cdot GTP}$ (I), $f_{Ras\cdot GTP}$ (II), and $f_{Ras\cdot GTP}$ (III) values of wt HRas. By setting the values of the GEF- and GAP-relevant kinetic terms for the calculation of the comprehensive $f_{Ras\cdot GTP}$ (I), $f_{Ras\cdot GTP}$ (II), and $f_{Ras\cdot GTP}$ (III) values of wt HRas as default values, we can predict via a comparison of these comprehensive $f_{Ras\cdot GTP}$ values of wt HRas with the cellular $f_{Ras\cdot GTP}$ values of wt HRas in unstimulated NIH 3T3 cells the status of SOS in unstimulated NIH 3T3 cells. For example, the estimated value of the cellular $f_{Ras\cdot GTP}$ of the transfected wt HRas in unstimulated NIH 3T3 cells (Figure 4) can be obtained by a value combination of ~80% of the minimally active 5 nM SOS with ~20% of the highly active 5 nM SOS with 10 nM p120GAP in eq 1. Nevertheless, direct measurements of the cellular expression levels and activities of GEFs and GAPs are necessary. Such measurements increase the likelihood of obtaining meaningful estimated percentages for the cellular expression levels and activities of SOS and p120GAP associated with the comprehensive $f_{Ras\cdot GTP}$ value of wt HRas.

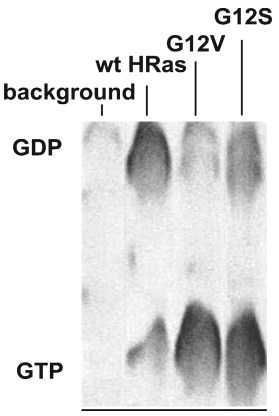

Figure 4. Determination of the fractions of HRas-bound GTP in cells. GTP fractions bound to various forms of Ras expressed in unstimulated NIH 3T3 cells were determined as described in Materials and Methods. Western blot analysis showed that all transfected Ras proteins were evenly expressed. The fraction values of Ras-bound GTP [[Ras·GTP]/([Ras·GTP] + [Ras·GDP])] using densitometry estimation of GTP and GDP concentrations were calculated: background (transfection of the mammalian expression vector without the *ras* gene), not determined; wt HRas, 0.12; G12V HRas, 0.81; G12S HRas, 0.62. The presented values are the averages of the values of the independent triplicate measurements using separate cell culture samples, and the SDs are less than 10% of the GTP fraction values that were indicated.

Note that the previous study also showed that the fraction of the cellular $f_{Ras\cdot GTP}$ value of the transfected wt HRas in unstimulated NIH 3T3 cells does not significantly differ from the cellular $f_{Ras\cdot GTP}$ value of the endogenous wt HRas in unstimulated NIH 3T3 cells.[34] This lack of a significant difference was found despite the expression level of the transfected wt HRas being much higher than that of the endogenous wt HRas in unstimulated NIH 3T3 cells. Hence, the analysis of the features of the cellular $f_{Ras\cdot GTP}$ value of the transfected wt HRas in unstimulated NIH 3T3 cells that was performed by using the comprehensive $f_{Ras\cdot GTP}$ (I), $f_{Ras\cdot GTP}$ (II), and $f_{Ras\cdot GTP}$ (III) values of wt HRas (see above) may reflect the cellular traits of the endogenous wt HRas. This endogenous wt

dx.doi.org/10.1021/bi400679q | *Biochemistry* 2013, 52, 8465−8479

HRas is associated with the cellular expression and activities of SOS and p120GAP in unstimulated NIH 3T3 cells.

Analysis of the Comprehensive $f_{Ras\cdot GTP}$ Values of HRas Mutants. To one degree or another, all of the values of the comprehensive $f_{Ras\cdot GTP}$ (I) of these HRas mutants exceeded the values of the comprehensive $f_{Ras\cdot GTP}$ (I) of wt HRas.

According to the main kinetic factor that changes the value of the comprehensive $f_{Ras\cdot GTP}$ (I) of Ras, the values of the comprehensive $f_{Ras\cdot GTP}$ (I) of the p-loop and NKCD/SAK HRas mutants can be divided into two types for purposes of comparison with the values of the comprehensive $f_{Ras\cdot GTP}$ (I) of wt HRas. First, the values of the GAP-relevant kinetic terms of HRas mutants in eq 1 are almost zero; as a consequence, the value of the comprehensive $f_{Ras\cdot GTP}$ (I) of HRas mutants is significantly large. Mechanically, such small values of the GAP-relevant kinetic terms of HRas mutants are rooted in the almost total impairment of the catalytic action of p120GAP on HRas mutants. The p-loop HRas mutants G12V and G13V possess this kinetic characteristic. Second, the higher values of the intrinsic kinetic terms of HRas mutants and/or the lower values of the GAP-relevant kinetic terms for HRas mutants, when compared with the values associated with wt HRas in eq 1, yield larger values of the comprehensive $f_{Ras\cdot GTP}$ (I) of HRas mutants compared to the value of the comprehensive $f_{Ras\cdot GTP}$ (I) of wt HRas. In all of these cases, these altered values are caused by the perturbed intrinsic kinetic processes of HRas mutants and/or GAP catalytic efficiencies on HRas mutants. With the exception of G12V and G13V HRas, all of the examined HRas mutants have this kinetic trait.

Similar to the case of the comprehensive $f_{Ras\cdot GTP}$ (I) of these HRas mutants, all of the values of the comprehensive $f_{Ras\cdot GTP}$ (II) of HRas mutants were higher under the same conditions versus the values of the comprehensive $f_{Ras\cdot GTP}$ of wt HRas (Table 4). On the basis of the main kinetic factor that contributes to altering the value of the comprehensive $f_{Ras\cdot GTP}$ (II) of Ras, the values of the comprehensive $f_{Ras\cdot GTP}$ (II) of the p-loop and NKCD/SAK HRas mutants fall into two categories upon comparison with the value of the comprehensive $f_{Ras\cdot GTP}$ (II) of wt HRas. First, the higher values of the intrinsic kinetic terms of these HRas mutants, in conjunction with the comparatively lower values of the catalytic efficiencies of p120GAP on these HRas mutants versus those of wt HRas, mainly contribute to give higher values for the comprehensive $f_{Ras\cdot GTP}$ (II) of HRas mutants than for the comprehensive $f_{Ras\cdot GTP}$ (II) of wt HRas. The perturbed intrinsic processes of HRas mutants and GAP catalytic efficiencies on HRas mutants are responsible for such value changes in the intrinsic kinetic terms and/or the GAP-relevant kinetic terms of HRas mutants. All p-loop HRas mutants, but not these NKCD/SAK HRas mutants, have this kinetic trait. Second, only a significantly high value of the intrinsic kinetic terms of HRas mutants, compared with those of wt HRas, contributes to the generation of higher values of the comprehensive $f_{Ras\cdot GTP}$ (II) of HRas mutants versus the comparative values of wt HRas. The significantly higher values of the intrinsic kinetic terms of HRas mutants, compared with those of wt HRas, are caused by the perturbed intrinsic processes of HRas mutants. In this case, no causation can be attributed to the change in the values of the catalytic efficiencies of p120GAP of HRas mutants. The NKCD/SAK HRas mutants, including K117R, A146T, and A146V, have this kinetic feature.

All values of the comprehensive $f_{Ras\cdot GTP}$ (III) of these HRas mutants are almost uniformly similar to the value of the comprehensive $f_{Ras\cdot GTP}$ (III) of wt HRas, which is extremely high (i.e., ≥0.87) (Table 4). This similarity exists because the value of the GEF-relevant kinetic terms (the value associated with the highly active 0.6 μM SOS) overwhelms all other kinetic parameters associated with the value of the GAP-relevant kinetic terms (the value associated with 10 nM p120GAP) and the intrinsic kinetic parameter values of Ras in eq 1. In addition, as discussed elsewhere, this highly active 0.6 μM SOS and 10 nM p120GAP condition can also generate an extremely high value for the comprehensive $f_{Ras\cdot GTP}$ of wt HRas. The highly active 0.6 μM SOS and 10 nM p120GAP generates significantly higher values for the comprehensive $f_{Ras\cdot GTP}$ (III) of Ras than it does for any examined HRas proteins. Because of these high values, it is certain that a cellular condition with the highly active 0.6 μM SOS and 10 nM p120GAP is sufficient to produce uncontrolled Ras-dependent cellular signaling events without regard to the values of any other examined HRas mutants or wt HRas.

G12S HRas is one of the most predominant forms found in Costello syndrome (Table 1).[35] Hence, the value of the cellular $f_{Ras\cdot GTP}$ of G12S HRas in unstimulated NIH 3T3 cells was determined as a way to use various combinations of activities and expression levels of SOS with p120GAP to evaluate the various comprehensive $f_{Ras\cdot GTP}$ values of G12S HRas. Because of the important role of G12V HRas in cancer formation, the cellular $f_{Ras\cdot GTP}$ value of G12V HRas in unstimulated NIH 3T3 cells also was determined to be a way to use various combinations of activities and expression levels of SOS with p120GAP to evaluate these various comprehensive $f_{Ras\cdot GTP}$ (I), $f_{Ras\cdot GTP}$ (II), and $f_{Ras\cdot GTP}$ (III) values of G12V HRas. The cellular $f_{Ras\cdot GTP}$ value of G12V HRas in unstimulated NIH 3T3 cells also serves as a positive control for the analysis of the cellular $f_{Ras\cdot GTP}$ value of G12S HRas in unstimulated NIH 3T3 cells. The value of the cellular $f_{Ras\cdot GTP}$ of wt HRas in unstimulated NIH 3T3 cells serves as a negative control for this analysis. The cellular $f_{Ras\cdot TP}$ values of G12V and G12S HRas in unstimulated NIH 3T3 cells were determined to be 0.80 and 0.63, respectively, which are ∼8.0- and 6.3-fold higher, respectively, than the cellular $f_{Ras\cdot GTP}$ value of wt HRas in unstimulated NIH 3T3 cells (Figure 4).

DISCUSSION

This study establishes novel kinetic parameter-based calculations of the values of the intrinsic, GEF- and GAP-mediated, and comprehensive $f_{Ras\cdot GTP}$ of Ras proteins that represent the cellular content of the GTP-bound form of Ras in the presence and absence of GEF and/or GAP. The kinetic characterizations linked with the calculations of the population of the GTP-bound form of Ras first provide an overall picture of the inherited causality between Ras mutations and changes in the cellular population of the GTP-bound Ras. These linkages explain the biochemical roles of these HRas mutants in various diseases. These roles include diseases such as Costello syndrome and certain cancers.

Depending on the cellular activity and expression of GEFs in combination with GAPs, three sets of values of the comprehensive $f_{Ras\cdot GTP}$ of Ras, the comprehensive $f_{Ras\cdot GTP}$ (I), $f_{Ras\cdot GTP}$ (II), and $f_{Ras\cdot GTP}$ (III) of these forms of HRas, were calculated. Comparison of these calculated values with the values of the cellular $f_{Ras\cdot GTP}$ of selected HRas proteins in the unstimulated NIH 3T3 cells suggests that the comprehensive $f_{Ras\cdot GTP}$ (I) values of HRas mainly represent the actual cellular $f_{Ras\cdot GTP}$ values of HRas in the unstimulated NIH 3T3 cells. This

dx.doi.org/10.1021/bi400679q | Biochemistry 2013, 52, 8465−8479

recognition takes into account the component of the comprehensive $f_{Ras\cdot GTP}$ (II) of HRas. Intriguingly, although there are no clear-cut dividing lines, the spectrum of the calculated values of the comprehensive $f_{Ras\cdot GTP}$ (I) of HRas mutants can be classified into three groups. The first group encompasses the values of 0.57−0.67 and is associated with G12V and G13V HRas mutants. The G12V and G13V mutations of HRas are the only ones linked specifically and exclusively to cancer formation. The second group spans 0.24−0.28 and is linked to G12A, G12S, G13S, and G13C mutations of HRas. These HRas mutations are mainly linked to the development of Costello syndrome, but they are also often linked to cancers. Finally, the third group has a range of 0.06−0.12 and is associated with all other listed HRas mutants. This group includes G12C, G12D, G12E, G13D, K117R, A146T, and A146V mutations of HRas that are linked only to the development of Costello syndrome. These groups and their links to cancer and/or Costello syndrome suggest that the high end of the spectrum of values of the comprehensive $f_{Ras\cdot GTP}$ (I) of HRas mutants is certainly linked to cancer formation, but the low end of this spectrum is associated only with the development of Costello syndrome. Values in the midrange of this spectrum are linked with the development of both of Costello syndrome and cancer. Accordingly, it is possible to postulate that the values of the comprehensive $f_{Ras\cdot GTP}$ (I) of HRas mutants can be used to gauge whether Ras mutants cause development of diseases such as cancers and/or Costello syndrome. For example, if a comprehensive $f_{Ras\cdot GTP}$ (I) value of a certain HRas mutant is 0.25, this HRas mutation is likely to cause the development of Costello syndrome and/or cancers. However, if the same value of a certain HRas mutant is 0.10, this HRas mutation is likely to lead only to the development of Costello syndrome. The cellular $f_{Ras\cdot GTP}$ values of HRas proteins from unstimulated NIH 3T3 cells were used as references for the analyses of the comprehensive $f_{Ras\cdot GTP}$ (I) values of HRas proteins. Therefore, the analytical results discussed above cannot be applied immediately to diseases associated with Ras mutations in other cells. Use of our results to gauge other diseases must await further evaluation of the comprehensive $f_{Ras\cdot GTP}$ (I) of HRas by using the cellular $f_{Ras\cdot GTP}$ values of HRas from various other cells.

As discussed in the Results, the reason for such a large spectrum of values for the comprehensive $f_{Ras\cdot GTP}$ (I) of HRas mutants G12V and G13V is the fact that the catalytic action of p120GAP on these HRas mutants is impaired. However, the middle and the lower end of this spectrum, which includes all of the HRas mutants of this study except G12V and G13V, reflects the perturbation of the intrinsic kinetic parameters of HRas mutants in combination with the partial perturbation of these mutants by the catalytic action of p120GAP. Accounting for the linkages between certain groups of the comprehensive $f_{Ras\cdot GTP}$ (I) values of these HRas mutants and certain types of diseases (see above), the features of the mechanical perturbation of these HRas mutants can be further linked to the type of disease with which they are associated. The severe impairment of the catalytic action of p120GAP on HRas mutants results in the high-end values of the comprehensive $f_{Ras\cdot GTP}$ (I) of Ras. These values at the upper end of the spectrum cause the development of cancers. The perturbation of the intrinsic kinetic parameters of HRas mutants in combination with the partial perturbation of HRas mutants by the catalytic action of p120GAP leads to values in the middle or low ranges of the spectrum. Values in these ranges are sufficient for development of cancers and/or Costello syndrome.

Earlier, the main factor in increases in the cellular population of the GTP-bound Ras was thought to be the impaired catalytic action of GAP on HRas, with HRas mutations as the culprits in the impairment. This outlook remains consistent with the values at the upper end of the spectrum of values of the comprehensive $f_{Ras\cdot GTP}$ (I) of the tumorigenic G12V and G13V HRas mutants. However, this study is the first to show that perturbation that these HRas mutations cause in the intrinsic kinetic properties of Ras also plays a key role in increases in the cellular population of GTP-bound HRas. This notion is supported by the middle and low-end spectrum of values of the comprehensive $f_{Ras\cdot GTP}$ (I) of HRas proteins. Values in these ranges of the spectrum include those of all of the listed HRas mutants, except G12V and G13V. One of the best examples of this is the value of the comprehensive $f_{Ras\cdot GTP}$ (I) of the G12S HRas mutant. This is intriguing because G12S HRas is the most prevalent form of HRas mutant found in patients with Costello syndrome.

The value of the comprehensive $f_{Ras\cdot GTP}$ (III) of Ras represents a case in which the population of the GTP-bound form of Ras exists under conditions of extreme SOS expression and activity in cells. Regardless of the features of the HRas mutants, the values of the comprehensive $f_{Ras\cdot GTP}$ (III) of these HRas mutants are significantly high. Intriguingly, the development of at least one case of Noonan syndrome has been linked to high cellular $f_{Ras\cdot GTP}$ values of wt KRas and wt NRas.[13] The high values encountered in this case are suspected to be the result of upregulation of SOS that was caused by mutations of the *sos1* gene.[13] This SOS upregulation-dependent development of Noonan syndrome can be explained by an incident in the calculation of the value of the comprehensive $f_{Ras\cdot GTP}$ value (III) of wt HRas that dovetails with high SOS activity and expression.

Because other GAPs, such as NF1, have not been included in these analyses, an assessment of the effect of p120GAP on the cellular population of the GTP-bound Ras through the action of these HRas mutations should not be overinterpreted. Moreover, no exploration of the possibility of a change in the p120GAP expression-dependent cellular population of the GTP-bound form of Ras that is associated with these HRas mutations has been undertaken. This limitation reflects the lack of evidence of higher or lower levels of cellular expression of p120GAP other than as 10 nM p120GAP. Future studies are expected to examine the possibility that the various cellular expressions of p120GAP as well as NF1 modulate the cellular population of these HRas mutations in the GTP-bound form of Ras.

■ ASSOCIATED CONTENT

Supporting Information

Derivation of eqs 1−4. This material is available free of charge via the Internet at http://pubs.acs.org.

■ AUTHOR INFORMATION

Corresponding Author

*Department of Chemistry and Biochemistry, The University of Texas at Arlington, 700 Planetarium Pl., Arlington, TX 76019. E-mail: jheo@uta.edu. Telephone: (817) 272-9627. Fax: (817) 272-3808.

Present Address

[‖]J.L.: Regenerative Medicine Research Center, Korea Research Institute of Bioscience and Biotechnology, 125 Gwahak-ro, Yuseong-gu, Daejeon 305-806, Korea.

Funding

This work was supported by National Institutes of Health Grant 1R15AI096146-01A1 to J.H.

Notes

The authors declare no competing financial interest.

■ ABBREVIATIONS

[GAP], GAP protein concentration; [GEF], GEF protein concentration; Cdc25, Ras SOS1 catalytic core domain; GAPs, GTPase-activating proteins; GEFs, guanine nucleotide exchange factors; GNE, guanine nucleotide exchange; HRas, Harvey Ras; KRas, Kirsten Ras; mantGDP, 2′(3′)-*O*-(*N*-methylanthraniloyl) guanosine diphosphate; mantGppNHp, 2′(3′)-*O*-(*N*-methylanthraniloyl) 5′-guanylyl-imidodiphosphate; NF1, neurofibromin1; NRas, Neuroblastoma Ras; RasGRF, Ras guanine nucleotide release factor; RasGRP, Ras guanyl nucleotide-releasing protein; SOS, Son of Sevenless; comprehensive $f_{Ras\cdot GTP}$ (I) of Ras, comprehensive $f_{Ras\cdot GTP}$ of Ras with the minimally active 5 nM SOS and 5 nM p120GAP; comprehensive $f_{Ras\cdot GTP}$ (II) of Ras, comprehensive $f_{Ras\cdot GTP}$ of Ras with the highly active 5 nM SOS and 5 nM p120GAP; comprehensive $f_{Ras\cdot GTP}$ (III) of Ras, comprehensive $f_{Ras\cdot GTP}$ of Ras with the highly active 0.6 μM SOS and 5 nM p120GAP; comprehensive $f_{Ras\cdot GTP}$, overall comprehensive cellular fraction of GTP-bound Ras over GTP- and GDP-bound Ras in the presence of GEF and GAP; GAP-mediated $f_{Ras\cdot GTP}$, cellular fraction of GTP-bound Ras over GTP- and GDP-bound Ras in the presence of GAP; GEF-mediated $f_{Ras\cdot GTP}$ (I) of Ras, GEF-mediated $f_{Ras\cdot GTP}$ of Ras with the minimally active 5 nM SOS; GEF-mediated $f_{Ras\cdot GTP}$ (II) of Ras, GEF-mediated $f_{Ras\cdot GTP}$ of Ras with the highly active 5 nM SOS; GEF-mediated $f_{Ras\cdot GTP}$ (III) of Ras, GEF-mediated $f_{Ras\cdot GTP}$ of Ras with the highly active 0.6 μM SOS; GEF-mediated $f_{Ras\cdot GTP}$, cellular fraction of GTP-bound Ras over GTP- and GDP-bound Ras in the presence of GEF; intrinsic $f_{Ras\cdot GTP}$, intrinsic cellular fraction of GTP-bound Ras over GTP- and GDP-bound Ras; wt, wild type.

■ REFERENCES

(1) Oxford, G., and Theodorescu, D. (2003) Ras superfamily monomeric G proteins in carcinoma cell motility. *Cancer Lett. 189*, 117−128.

(2) Marshall, C. B., Meiri, D., Smith, M. J., Mazhab-Jafari, M. T., Gasmi-Seabrook, G. M. C., Rottapel, R., Stambolic, V., and Ikura, M. (2012) Probing the GTPase cycle with real-time NMR: GAP and GEF activities in cell extracts. *Methods 57*, 473−485.

(3) Geyer, M., and Wittinghofer, A. (1997) GEFs, GAPs, GDIs and effectors: Taking a closer (3D) look at the regulation of Ras-related GTP-binding proteins. *Curr. Opin. Struct. Biol. 7*, 786−792.

(4) Bonfini, L., Karlovich, C. A., Dasgupta, C., and Banerjee, U. (1992) The Son of sevenless gene product: A putative activator of Ras. *Science 255*, 603−606.

(5) Ebinu, J. O., Bottorff, D. A., Chan, E. Y., Stang, S. L., Dunn, R. J., and Stone, J. C. (1998) RasGRP, a Ras guanyl nucleotide-releasing protein with calcium- and diacylglycerol-binding motifs. *Science 280*, 1082−1086.

(6) Bottorff, D., Ebinu, J., and Stone, J. C. (1999) RasGRP, a Ras activator: Mouse and human cDNA sequences and chromosomal positions. *Mamm. Genome 10*, 358−361.

(7) Boriack-Sjodin, P. A., Margarit, S. M., Bar-Sagi, D., and Kuriyan, J. (1998) The structural basis of the activation of Ras by Sos. *Nature 394*, 337−343.

(8) Traut, T. W. (1994) Physiological concentrations of purines and pyrimidines. *Mol. Cell. Biochem. 140*, 1−22.

(9) Sprang, S. (2001) GEFs: Master regulators of G-protein activation. *Trends Biochem. Sci. 26*, 266−267.

(10) Grewal, T., Koese, M., Tebar, F., and Enrich, C. (2011) Differential Regulation of RasGAPs in Cancer. *Genes Cancer 2*, 288−297.

(11) Scheffzek, K., Ahmadian, M. R., Kabsch, W., Wiesmuller, L., Lautwein, A., Schmitz, F., and Wittinghofer, A. (1997) The Ras-RasGAP complex: Structural basis for GTPase activation and its loss in oncogenic Ras mutants. *Science 277*, 333−338.

(12) Boguski, M. S., and McCormick, F. (1993) Proteins regulating Ras and its relatives. *Nature 366*, 643−654.

(13) Schubbert, S., Shannon, K., and Bollag, G. (2007) Hyperactive Ras in developmental disorders and cancer. *Nat. Rev. Cancer 7*, 295−308.

(14) Roberts, P. J., and Der, C. J. (2007) Targeting the Raf-MEK-ERK mitogen-activated protein kinase cascade for the treatment of cancer. *Oncogene 26*, 3291−3310.

(15) Fasano, O., Aldrich, T., Tamanoi, F., Taparowsky, E., Furth, M., and Wigler, M. (1984) Analysis of the transforming potential of the human H-ras gene by random mutagenesis. *Proc. Natl. Acad. Sci. U.S.A. 81*, 4008−4012.

(16) Matsuda, K., Shimada, A., Yoshida, N., Ogawa, A., Watanabe, A., Yajima, S., Iizuka, S., Koike, K., Yanai, F., Kawasaki, K., Yanagimachi, M., Kikuchi, A., Ohtsuka, Y., Hidaka, E., Yamauchi, K., Tanaka, M., Yanagisawa, R., Nakazawa, Y., Shiohara, M., Manabe, A., and Kojima, S. (2007) Spontaneous improvement of hematologic abnormalities in patients having juvenile myelomonocytic leukemia with specific RAS mutations. *Blood 109*, 5477−5480.

(17) Jakubauskas, A., and Griskevicius, L. (2010) KRas and BRaf mutational status analysis from formalin-fixed, paraffin-embedded tissues using multiplex polymerase chain reaction-based assay. *Arch. Pathol. Lab. Med. 134*, 620−624.

(18) Sahu, R. P., Batra, S., Kandala, P. K., Brown, T. L., and Srivastava, S. K. (2011) The role of K-ras gene mutation in TRAIL-induced apoptosis in pancreatic and lung cancer cell lines. *Cancer Chemother. Pharmacol. 67*, 481−487.

(19) Seeburg, P. H., Colby, W. W., Capon, D. J., Goeddel, D. V., and Levinson, A. D. (1984) Biological properties of human c-Ha-ras1 genes mutated at codon 12. *Nature 312*, 71−75.

(20) Hall, A., and Self, A. J. (1986) The effect of Mg^{2+} on the guanine nucleotide exchange rate of p21N-ras. *J. Biol. Chem. 261*, 10963−10965.

(21) Gideon, P., John, J., Frech, M., Lautwein, A., Clark, R., Scheffler, J. E., and Wittinghofer, A. (1992) Mutational and kinetic analyses of the GTPase-activating protein (GAP)-p21 interaction: The C-terminal domain of GAP is not sufficient for full activity. *Mol. Cell. Biol. 12*, 2050−2056.

(22) Lenzen, C., Cool, R. H., Prinz, H., Kuhlmann, J., and Wittinghofer, A. (1998) Kinetic analysis by fluorescence of the interaction between Ras and the catalytic domain of the guanine nucleotide exchange factor $Cdc25^{Mm}$. *Biochemistry 37*, 7420−7430.

(23) Cotton, F. A., and Wilkinson, G. (1988) *Advanced Inorganic Chemistry*, 5th ed., John Wiley & Sons, New York.

(24) Heo, J., and Campbell, S. L. (2005) Superoxide Anion Radical Modulates the Activity of Ras and Ras-related GTPases by a Radical-based Mechanism Similar to that of Nitric Oxide. *J. Biol. Chem. 280*, 12438−12445.

(25) Leupold, C. M., Goody, R. S., and Wittinghofer, A. (1983) Stereochemistry of the elongation factor Tu X GTP complex. *Eur. J. Biochem. 135*, 237−241.

(26) Eccleston, J. F., Moore, K. J., Morgan, L., Skinner, R. H., and Lowe, P. N. (1993) Kinetics of interaction between normal and proline 12 Ras and the GTPase-activating proteins, p120-GAP and neurofibromin. The significance of the intrinsic GTPase rate in

determining the transforming ability of ras. *J. Biol. Chem. 268*, 27012−27019.
(27) Downward, J., Graves, J. D., Warne, P. H., Rayter, S., and Cantrell, D. A. (1990) Stimulation of p21ras upon T-cell activation. *Nature 346*, 719−723.
(28) Krengel, U., Schlichting, I., Scherer, A., Schumann, R., Frech, M., John, J., Kabsch, W., Pai, E. F., and Wittinghofer, A. (1990) Three-dimensional structures of H-ras p21 mutants: Molecular basis for their inability to function as signal switch molecules. *Cell 62*, 539−548.
(29) John, J., Frech, M., and Wittinghofer, A. (1988) Biochemical properties of Ha-ras encoded p21 mutants and mechanism of the autophosphorylation reaction. *J. Biol. Chem. 263*, 11792−11799.
(30) Maurer, T., Garrenton, L. S., Oh, A., Pitts, K., Anderson, D. J., Skelton, N. J., Fauber, B. P., Pan, B., Malek, S., Stokoe, D., Ludlam, M. J., Bowman, K. K., Wu, J., Giannetti, A. M., Starovasnik, M. A., Mellman, I., Jackson, P. K., Rudolph, J., Wang, W., and Fang, G. (2012) Small-molecule ligands bind to a distinct pocket in Ras and inhibit SOS-mediated nucleotide exchange activity. *Proc. Natl. Acad. Sci. U.S.A. 109*, 5299−5304.
(31) Kuniba, H., Pooh, R. K., Sasaki, K., Shimokawa, O., Harada, N., Kondoh, T., Egashira, M., Moriuchi, H., Yoshiura, K., and Niikawa, N. (2009) Prenatal diagnosis of Costello syndrome using 3D ultrasonography amniocentesis confirmation of the rare HRAS mutation G12D. *Am. J. Med. Genet., Part A 149*, 785−787.
(32) Gureasko, J., Galush, W. J., Boykevisch, S., Sondermann, H., Bar-Sagi, D., Groves, J. T., and Kuriyan, J. (2008) Membrane-dependent signal integration by the Ras activator Son of sevenless. *Nat. Struct. Mol. Biol. 15*, 452−461.
(33) Bollag, G., and McCormick, F. (1991) Differential regulation of rasGAP and neurofibromatosis gene product activities. *Nature 351*, 576−579.
(34) Scheele, J. S., Rhee, J. M., and Boss, G. R. (1995) Determination of absolute amounts of GDP and GTP bound to Ras in mammalian cells: Comparison of parental and Ras-overproducing NIH 3T3 fibroblasts. *Proc. Natl. Acad. Sci. U.S.A. 92*, 1097−1100.
(35) Gelb, B. D., and Tartaglia, M. (2006) Noonan syndrome and related disorders: Dysregulated RAS-mitogen activated protein kinase signal transduction. *Hum. Mol. Genet. 15* (Special Issue 2), R220−R226.
(36) Aoki, Y., Niihori, T., Kawame, H., Kurosawa, K., Ohashi, H., Tanaka, Y., Filocamo, M., Kato, K., Suzuki, Y., Kure, S., and Matsubara, Y. (2005) Germline mutations in HRAS proto-oncogene cause Costello syndrome. *Nat. Genet. 37*, 1038−1040.
(37) Gripp, K. W., Lin, A. E., Stabley, D. L., Nicholson, L., Scott, C. I., Jr., Doyle, D., Aoki, Y., Matsubara, Y., Zackai, E. H., Lapunzina, P., Gonzalez-Meneses, A., Holbrook, J., Agresta, C. A., Gonzalez, I. L., and Sol-Church, K. (2006) HRAS mutation analysis in Costello syndrome: Genotype and phenotype correlation. *Am. J. Med. Genet., Part A 140*, 1−7.
(38) Estep, A. L., Tidyman, W. E., Teitell, M. A., Cotter, P. D., and Rauen, K. A. (2006) HRAS mutations in Costello syndrome: Detection of constitutional activating mutations in codon 12 and 13 and loss of wild-type allele in malignancy. *Am. J. Med. Genet., Part A 140*, 8−16.
(39) Kerr, B., Delrue, M. A., Sigaudy, S., Perveen, R., Marche, M., Burgelin, I., Stef, M., Tang, B., Eden, O. B., O'Sullivan, J., De Sandre-Giovannoli, A., Reardon, W., Brewer, C., Bennett, C., Quarell, O., M'Cann, E., Donnai, D., Stewart, F., Hennekam, R., Cave, H., Verloes, A., Philip, N., Lacombe, D., Levy, N., Arveiler, B., and Black, G. (2006) Genotype-phenotype correlation in Costello syndrome: HRAS mutation analysis in 43 cases. *J. Med. Genet. 43*, 401−405.
(40) Sol-Church, K., Stabley, D. L., Nicholson, L., Gonzalez, I. L., and Gripp, K. W. (2006) Paternal bias in parental origin of HRAS mutations in Costello syndrome. *Hum. Mutat. 27*, 736−741.
(41) Zampino, G., Pantaleoni, F., Carta, C., Cobellis, G., Vasta, I., Neri, C., Pogna, E. A., De Feo, E., Delogu, A., Sarkozy, A., Atzeri, F., Selicorni, A., Rauen, K. A., Cytrynbaum, C. S., Weksberg, R., Dallapiccola, B., Ballabio, A., Gelb, B. D., Neri, G., and Tartaglia, M. (2007) Diversity, parental germline origin, and phenotypic spectrum of de novo HRAS missense changes in Costello syndrome. *Hum. Mutat. 28*, 265−272.
(42) van der Burgt, I., Kupsky, W., Stassou, S., Nadroo, A., Barroso, C., Diem, A., Kratz, C. P., Dvorsky, R., Ahmadian, M. R., and Zenker, M. (2007) Myopathy caused by HRAS germline mutations: Implications for disturbed myogenic differentiation in the presence of constitutive HRas activation. *J. Med. Genet. 44*, 459−462.
(43) Gripp, K. W., Innes, A. M., Axelrad, M. E., Gillan, T. L., Parboosingh, J. S., Davies, C., Leonard, N. J., Lapointe, M., Doyle, D., Catalano, S., Nicholson, L., Stabley, D. L., and Sol-Church, K. (2008) Costello syndrome associated with novel germline HRAS mutations: An attenuated phenotype? *Am. J. Med. Genet., Part A 146*, 683−690.
(44) Burkitt-Wright, E. M., Bradley, L., Shorto, J., McConnell, V. P., Gannon, C., Firth, H. V., Park, S. M., D'Amore, A., Munyard, P. F., Turnpenny, P. D., Charlton, A., Wilson, M., and Kerr, B. (2012) Neonatal lethal Costello syndrome and unusual dinucleotide deletion/insertion mutations in HRAS predicting p.Gly12Val. *Am. J. Med. Genet., Part A 158*, 1102−1110.
(45) Niihori, T., Aoki, Y., Okamoto, N., Kurosawa, K., Ohashi, H., Mizuno, S., Kawame, H., Inazawa, J., Ohura, T., Arai, H., Nabatame, S., Kikuchi, K., Kuroki, Y., Miura, M., Tanaka, T., Ohtake, A., Omori, I., Ihara, K., Mabe, H., Watanabe, K., Niijima, S., Okano, E., Numabe, H., and Matsubara, Y. (2011) HRAS mutants identified in Costello syndrome patients can induce cellular senescence: Possible implications for the pathogenesis of Costello syndrome. *J. Hum. Genet. 56*, 707−715.
(46) Digilio, M. C., Lepri, F., Baban, A., Dentici, M. L., Versacci, P., Capolino, R., Ferese, R., De Luca, A., Tartaglia, M., Marino, B., and Dallapiccola, B. (2011) RASopathies: Clinical Diagnosis in the First Year of Life. *Mol. Syndromol. 1*, 282−289.
(47) Tidyman, W. E., Lee, H. S., and Rauen, K. A. (2011) Skeletal muscle pathology in Costello and cardio-facio-cutaneous syndromes: Developmental consequences of germline Ras/MAPK activation on myogenesis. *Am. J. Med. Genet., Part C 157*, 104−114.
(48) Gripp, K. W., Hopkins, E., Sol-Church, K., Stabley, D. L., Axelrad, M. E., Doyle, D., Dobyns, W. B., Hudson, C., Johnson, J., Tenconi, R., Graham, G. E., Sousa, A. B., Heller, R., Piccione, M., Corsello, G., Herman, G. E., Tartaglia, M., and Lin, A. E. (2011) Phenotypic Analysis of Individuals With Costello Syndrome due to HRAS p.G13C. *Am. J. Med. Genet., Part A 155*, 706−716.
(49) Piccione, M., Piro, E., Pomponi, M. G., Matina, F., Pietrobono, R., Candela, E., Gabriele, B., Neri, G., and Corsello, G. (2009) A Premature Infant With Costello Syndrome Due to a Rare G13C HRAS Mutation. *Am. J. Med. Genet., Part A 149*, 487−489.
(50) Schulz, A. L., Albrecht, B., Arici, C., van der Burgt, I., Buske, A., Gillessen-Kaesbach, G., Heller, R., Horn, D., Hubner, C. A., Korenke, G. C., Konig, R., Kress, W., Kruger, G., Meinecke, P., Mucke, J., Plecko, B., Rossier, E., Schinzel, A., Schulze, A., Seemanova, E., Seidel, H., Spranger, S., Tuysuz, B., Uhrig, S., Wieczorek, D., Kutsche, K., and Zenker, M. (2008) Mutation and phenotypic spectrum in patients with cardio-facio-cutaneous and Costello syndrome. *Clin. Genet. 73*, 62−70.
(51) Denayer, E., Parret, A., Chmara, M., Schubbert, S., Vogels, A., Devriendt, K., Frijns, J. P., Rybin, V., de Ravel, T. J., Shannon, K., Cools, J., Scheffzek, K., and Legius, E. (2008) Mutation analysis in Costello syndrome: Functional and structural characterization of the HRAS p.Lys117Arg mutation. *Hum. Mutat. 29*, 232−239.
(52) Sinico, M., Bassez, G., Touboul, C., Cave, H., Vergnaud, A., Zirah, C., Fleury-Feith, J., Gettler, S., Vojtek, A. M., Chevalier, N., Amram, D., Alsamad, I. A., Haddad, B., and Encha-Razavi, F. (2011) Excess of neuromuscular spindles in a fetus with Costello syndrome: A clinicopathological report. *Pediatr. Dev. Pathol. 14*, 218−223.
(53) Piispanen, A. E., Bonnefoi, O., Carden, S., Deveau, A., Bassilana, M., and Hogan, D. A. (2011) Roles of Ras1 membrane localization during *Candida albicans* hyphal growth and farnesol response. *Eukaryotic Cell 10*, 1473−1484.
(54) Franken, S. M., Scheidig, A. J., Krengel, U., Rensland, H., Lautwein, A., Geyer, M., Scheffzek, K., Goody, R. S., Kalbitzer, H. R., Pai, E. F., et al. (1993) Three-dimensional structures and properties of

a transforming and a nontransforming glycine-12 mutant of p21H-ras. *Biochemistry 32*, 8411−8420.
(55) Gibbs, J. B., Schaber, M. D., Allard, W. J., Sigal, I. S., and Scolnick, E. M. (1988) Purification of ras GTPase activating protein from bovine brain. *Proc. Natl. Acad. Sci. U.S.A. 85*, 5026−5030.
(56) Feig, L. A., and Cooper, G. M. (1988) Relationship among guanine nucleotide exchange, GTP hydrolysis, and transforming potential of mutated ras proteins. *Mol. Cell. Biol. 8*, 2472−2478.